International Journal of Nanomedicine

Dovepress
open access to scientific and medical research

Open Access Full Text Article

ORIGINAL RESEARCH

Sustained-release nanoART formulation for the treatment of neuroAIDS

This article was published in the following Dove Press journal:
International Journal of Nanomedicine
4 February 2015
Number of times this article has been viewed

Rahul Dev Jayant
Venkata SR Atluri
Marisela Agudelo
Vidya Sagar
Ajeet Kaushik
Madhavan Nair

Center for Personalized Nanomedicine, Department of Immunology, Herbert Wertheim College of Medicine, Florida International University, Miami, FL, USA

Abstract: A novel approach was developed for the coencapsulation of an anti-HIV drug (tenofovir) and a latency-breaking agent (vorinostat), using magnetically guided layer-by-layer (LbL) assembled nanocarriers for the treatment of neuroAIDS. Ultrasmall iron oxide (Fe_3O_4) nanoparticles (10±3 nm) were synthesized and characterized. The LbL technique was used to achieve a sustained release profile, and application of 2 bilayers ([tenofovir+dextran sulphate]$_2$+vorinostat) to magnetic nanoparticles resulted in a 2.8 times increase in drug (tenofovir) loading and also resulted in an increase in the drug release period by 30-fold, with 100% drug release in sustained manner over a period of 5 days with the simultaneous stimulation of latent HIV expression. Nanoformulation showed a good blood–brain barrier transmigration ability (37.95%±1.5%) with good in vitro antiviral efficacy (~33% reduction of p24 level) over a period of 5 days after HIV infection in primary human astrocytes, with good cell viability (>90%). Hence, LbL arrangements of drugs on magnetic nanoparticles provides sustained release and, therefore, may improve the patient's adherence to therapy and lead to better compliance.

Keywords: layer-by-layer, magnetic nanocarriers, blood–brain barriers, neuroAIDS, sustained release, anti-HIV drug, latency

Introduction

Ever since the introduction of combination antiretroviral therapy (ART), HIV-infection-related morbidity and mortality have dramatically decreased. However, none of the currently available antiretroviral agents provides a cure. HIV infection has now become a chronic disease requiring a lifelong commitment to daily oral treatment.[1] Highly active ART (HAART) comprises complex regimens that require strict adherence to complicated treatment schedules, and the quality of treatment depends on the patient's adherence to the recommended regimens. Antiretroviral adherence is the second strongest predictor of progression to AIDS and death, after CD4 count.[2,3] Incomplete adherence to ART, however, is common in all groups of treated individuals. The average rate of adherence to ART is approximately 70%, despite the fact that long-term viral suppression requires near-perfect adherence.[4,5] Most antiretroviral drugs have a short half-life and, in turn, need be in circulation constantly to control the virus replication. It is believed that missing a medication dose even once can provide an opportunity for viruses to replicate such that a medication-resistant HIV strain may develop. Patient nonadherence can be a pervasive threat to health and well-being and can carry an appreciable economic burden. Despite all the best intentions and efforts on the part of health care professionals, a patient's noncompliance in the case of HIV therapy (HAART) is very high.[4] As per clinical trial data on HIV drugs, results show that missed doses of antiretroviral agents were most likely to occur because of forgetting (43%), sleeping through a dose (36%), being away from home (32%), changing

Correspondence: Rahul Dev Jayant
Center for Personalized Nanomedicine, Department of Immunology, Herbert Wertheim College of Medicine, Florida International University, 11200 SW 8th St., University Park, AHC-1, Miami, FL-33199, USA
Email rjayant@fiu.edu

Madhavan Nair
Center for Personalized Nanomedicine, Department of Immunology, Herbert Wertheim College of Medicine, Florida International University, 11200 SW 8th St., University Park, AHC-1, Miami, FL-33199, USA
Tel +1 305 348 1493
Fax +1 305 348 6021
Email nairm@fiu.edu

one's routine (27%), being too busy to take the dose (22%), feeling sick (11%), and experiencing depression (9%).[5,6] These shortfalls of nonadherence have serious and detrimental effects from the perspective of disease management and treatment.[7] Although no single intervention strategy can improve the adherence of all patients in HIV, and attempts to improve patient adherence depend on a set of key factors, reduction of dosing frequency can lead to efficient patient compliance.

HAART only helps in suppressing HIV replication, but it does not clear virus from infected individuals. Various reservoirs of replication-competent HIV have been identified that may contribute to this persistence. Several attempts have been made to clear the latent HIV reservoir, but these attempts have not been successful in eliminating all latently infected cells or in preventing virus rebound on cessation of therapy.[8] In addition, efforts should be made to target hidden latent virus in the body's sanctuaries, such as the brain, which serves as one of the sources of virus production to the periphery. Vorinostat, a histone deacetylase inhibitor, has shown great promise to break latency in $CD4^+$ T cells, and recent studies also have shown that other agents (tumor necrosis factor, interleukin 1β, and bryostatin) are being used as HIV-reactivating agents to break latency; nevertheless, the effect of vorinostat on the neuronal reservoir has not yet been established.[9,10] Scientists are exploring a variety of strategies in the hope of either completely eradicating HIV from the body (a sterilizing cure) or reducing it to such a low level that the immune system can maintain control without antiretroviral drugs (a functional cure). Among these strategies are agents that flush HIV out of latent reservoirs, drugs that keep hidden virus permanently inactive, and immune-strengthening therapies that protect cells from infection. The general scientific consensus is that a cure will likely require a combination approach. In spite of significant advances in HAART, the elimination of HIV-1 reservoirs from the central nervous system remains a formidable task.[11–13] This is mainly attributed to the inability of ART to penetrate the blood–brain barrier (BBB) and deprived the brain from the drug effects.[10,14–16] Long-acting formulations of therapeutic agents have been used to improve adherence and prevent issues such as missing doses or treatment fatigue to prescribed medication in a number of different fields such as contraception, male hypogonadism, and schizophrenia, with demonstrable success.[17] Therefore, as suggested earlier, the sustained release formulation of latency-breaking agents, together with antiretroviral drugs, could serve a multifunctional purpose and help eradicate HIV. Where sustained drug release may cause reduced adherence, a combination of latency-breaking and anti-HIV agents could eradicate a viral reservoir. The practice of nanotechnology in nanomedicine has shown exciting prospects for the development of a novel drug delivery system to achieve the desired therapeutic levels of anti-HIV drugs and HIV-reactivating agents across the BBB.[18–21] In a nutshell, we need to deliver the drugs across the brain, activate the latent HIV, and subsequently release HIV drugs from the carrier at a constant rate for a longer period to increase therapeutic adherence and eradicate the activated HIV reservoir without hampering the integrity of the BBB. Considering these scenarios, we have developed a novel, nanoengineered layer-by-layer (LbL) assembly of an anti-HIV drug (tenofovir) and a latency-breaking agent (vorinostat) on ultrasmall magnetic nanoparticles (MNPs) to achieve the sustained release of the drug for 5–7 days. The movement of MNPs can be "remote controlled" for its effective penetration across the BBB by applying an external magnetic force, as shown in the schematic in Figure 1.

Complementarily, LbL arrangements of drugs on MNPs will provide sustained release, therefore improving bioavailability and the patient's adherence to medication. The formulation assembly and underlying drug release mechanism from nanoengineered assembled MNP is represented in Figure 2.

Our current work is a proof-of-concept study demonstrating that an HIV latency-breaking agent (vorinostat) can be packaged into nanoparticles in conjunction with an antiretroviral drug (tenofovir). We have designed a formulation that uses nanotechnology to simultaneously reactivate and kill HIV in a sustained manner for 5 days across the BBB, which will be beneficial for the treatment of neuroAIDS. Therefore, our work provides a platform for more effective HIV therapy and possible future eradication of the virus.

Materials and methods

Synthesis of ultrasmall MNPs

The ultrasmall Fe_3O_4 MNPs were synthesized according to the coprecipitation method proposed by Sun et al[22] with minor modifications. All glassware was cleaned overnight by aqua regia before being used for the reactions. Briefly, a solution of 3 mL $FeCl_3$ (0.487 g dissolved in 2 mol/L HCl) and 10.33 mL H_2O was stir-mixed with 2 mL Na_2SO_3 (0.126 g in 2 mL of water) drop by drop over the course of a minute. On the change in color from yellow to red-light yellow, this solution was mixed into 80 mL NH_3+H_2O (0.85 mol/L) under vigorous stirring. A black precipitant quickly formed,

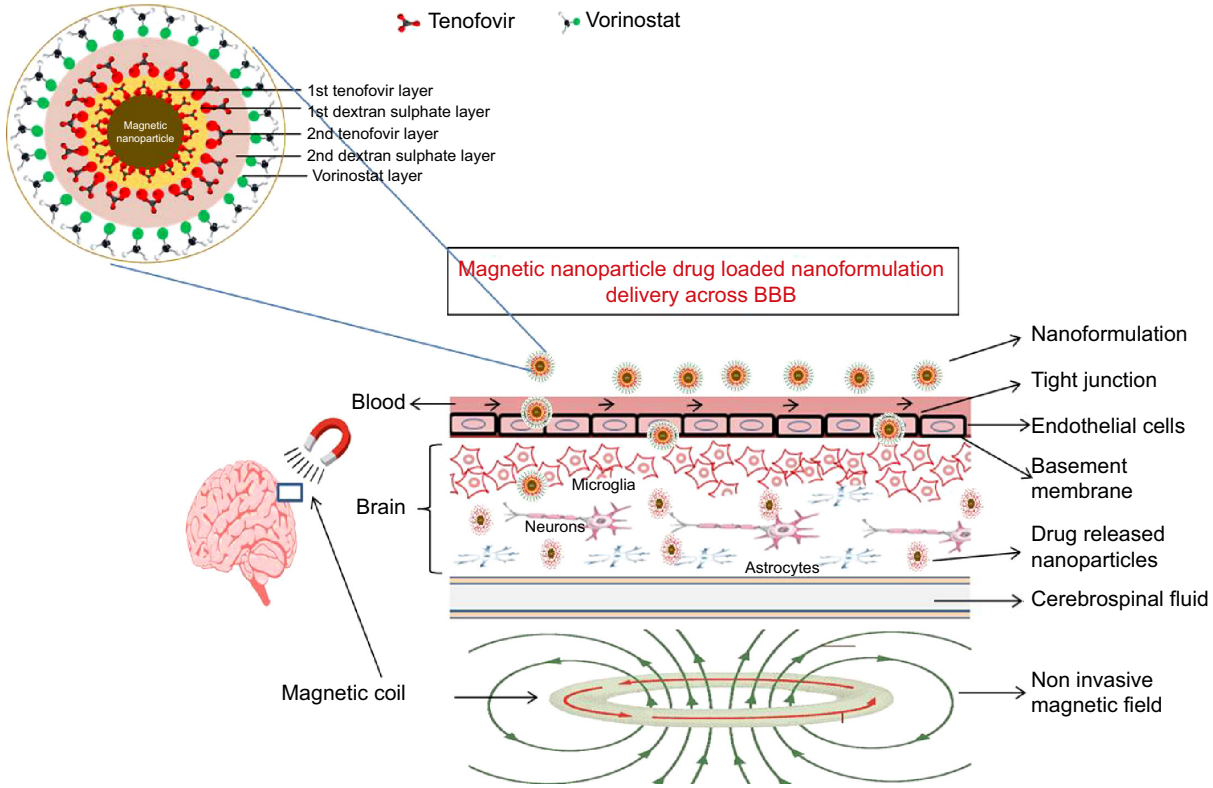

Figure 1 Nanoformulation delivery across the blood–brain barrier (BBB).
Notes: Proposed schematic of magnetic nanoparticle-based antiretroviral drug delivery across the BBB under the influence of an external noninvasive magnetic force.

which was allowed to crystallize further, for approximately 30 minutes, under continuous stirring. The suspension was washed, and formation of stable MNPs was achieved by adjusting the pH from 3.0 to 7.5 and the temperature from 90°C for first 5 minutes to 100°C for about 1 hour. A change in color from black to reddish-brown suggests the formation of compact MNPs, which are washed with water at least three times by the decantation method.

Characterization of MNPs and drug efficiency: X-ray diffraction and transmission electron microscopy analysis

Structural conformation of MNPs was determined by Shimadzu XRD-7000 diffractometer (Shimazdu, Tokyo, Japan). Transmission electron microscopy of MNPs was performed with the Phillips CM-200 200 kV transmission electron microscope operated at 80 kV. In brief, one drop of MNPs was spread on carbon support film on 400 mesh Cu grids (type B; Ted Pella, Inc., Redding, CA, USA). For better contrast during transmission electron microscopy imaging, samples on the grid were negatively stained with phosphotungstic acid (2.0% w/v; pH 6.4) and dried at room temperature. The size distribution and surface charge measurement of MNPs were carried out at 25°C in dynamic laser scattering (Zetasizer NanoZS, Malvern). The measurement of super paramagnetism was carried out by a classical vibrating sample magnetometer (Model 4 HF VSM, ADE, Lowell, MA, USA). The magnetic hysteresis loops of the Fe_3O_4 particles were measured between +1,200 and −1,200 Oersted at room temperature.

Time kinetics and drug-binding isotherm on MNPs

For determining the time kinetics of direct binding of tenofovir on MNPs, 1 mg/mL tenofovir solution to 1 mg MNPs was incubated in PBS buffer (pH 7.4) for 0.5, 1, 1.5, and 2 hours at room temperature. The amount of bound drug or percentage binding to the MNPs was determined by estimating the concentration of tenofovir in unbound fraction (supernatant) of the mixture by the spectrophotometric method at an ultraviolet absorbance of 260 nm. In addition, the effect of different drug concentrations (1–4 mg/mL) with respect to drug binding was calculated. For vorinostat, time kinetics and percentage drug binding were calculated as described earlier, and calculated using ultraviolet spectrophotometry at of 240 nm.

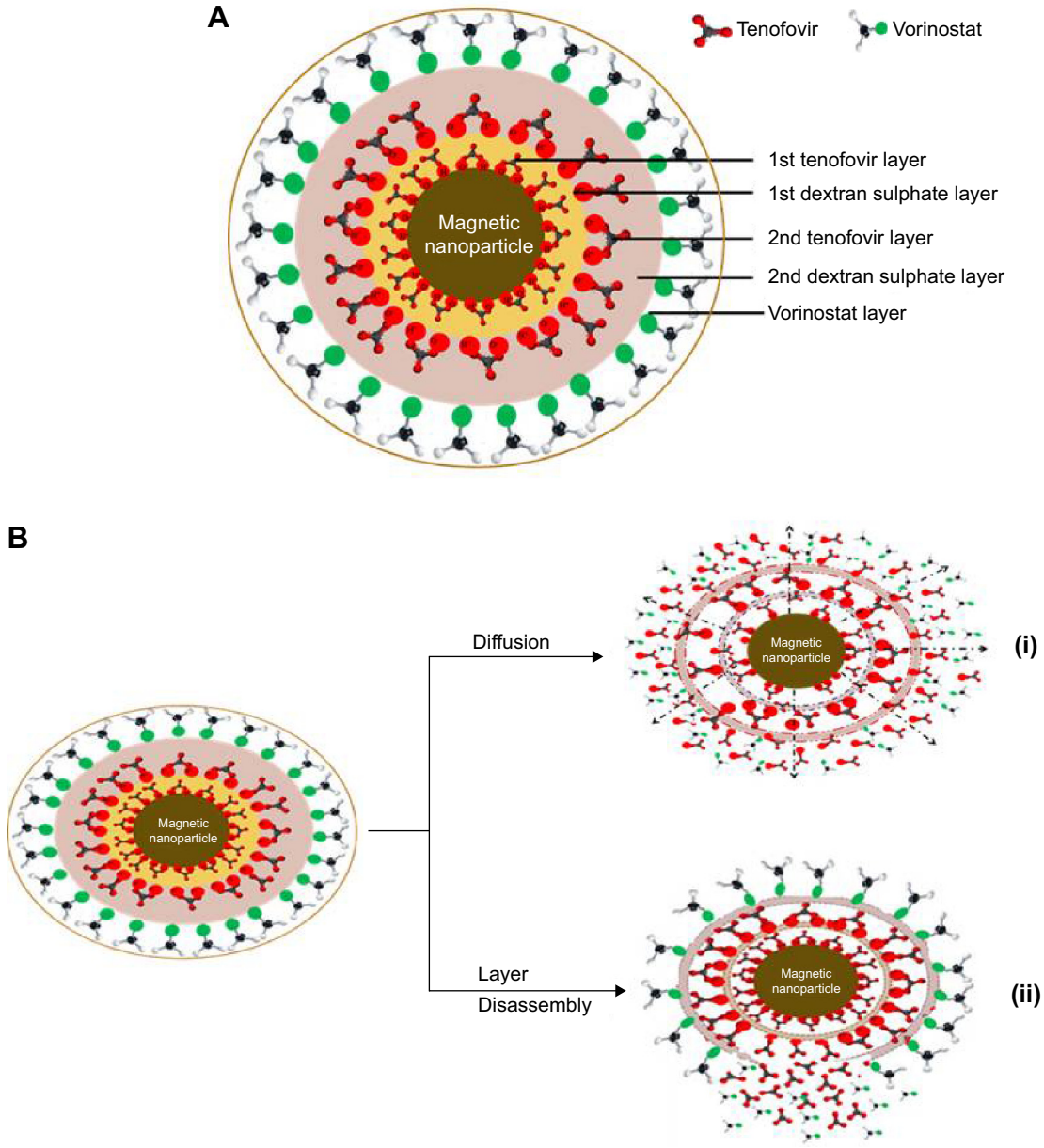

Figure 2 Formulation assembly and drug release mechanism.
Notes: (**A**) Schematic representation of formulation design. (**B**) Simplified illustration of the drug release mechanism from magnetic layer-by-layer assembled nanocarriers. (**i**) Diffusion-based drug release through pores. (**ii**) Drug release via surface hydrolysis of polymer chains of polyelectrolyte assembly.

LbL coatings on nanocarriers

A nanoengineered LbL self-assembly technique was used for nanoparticle coatings, as described by Decher.[23] The polyelectrolyte pairs used for this experiment were dextran sulphate (polyanion: 2 mg/mL in 0.15 M NaCl; molecular weight, 500,000) and tenofovir (polycation: 1 mg/mL in PBS; molecular weight, 287.213 g/mol). In brief, a solution of 2 mg/mL concentration of dextran sulphate sodium (DS) was prepared with 0.15 M NaCL, with pH adjusted to 7.4. For the coating, 100 µL DS was added to 1 mg drug-loaded MNPs and kept at room temperature for 20 minutes with intermittent shaking. The nanoparticles were then centrifuged at 2,500 rpm for 3 minutes to separate them from the unreacted DS solution and were washed with Milli-Q water. Later, 100 µL (1 mg/mL) positively charged drug (ie, tenofovir) was added for second-layer deposition to nanocarriers and held for 20 minutes of intermittent shaking. Finally, coated nanocarriers were washed twice with distilled water, using centrifugation. A similar process can be repeated two times to have 2 bilayer coatings on MNPs, and the surface charge of the MNPs was measured, using the zeta potential analyzer, after rinsing and before the addition of each layer. Finally, a vorinostat

(concentration, 0.05 mg/mL) layer was deposited to a bilayer (tenofovir+DS)$_2$ system. The final assembled nanoformulation was washed with distilled water, using centrifugation, and used for release studies.

In vitro drug release pharmacokinetic study

In vitro drug release studies were performed on uncoated MNPs and polyelectrolyte-coated assembled nanoformulation. Drug-loaded uncoated and coated MNP formulations were transferred to an Eppendorf tube containing 150 µL 0.01 M PBS buffer (pH 7.4). The samples were incubated at 37°C in an incubator, and at preset interval times (every 15 minutes), the release medium was collected and replaced with fresh buffer solution to maintain the sink condition. The cumulative percentage drug release data were obtained using amount of drug release from the total drug content and was determined spectrophotometrically at a λ_{max} of 260 and 240 nm for tenofovir and vorinostat, respectively. Statistical analysis of the data was performed using analysis of variance (single factor). Difference was considered significant when $P<0.05$.

Intracellular uptake analysis

Primary human astrocytes (HAs) were seeded on cover slips in six-well plates with a concentration of 1×10^6 cells. After 24 hours, cells were treated with an equal quantity of nanoformulation in the presence and/or absence of external magnetic forces for 6 hours. Cells were rinsed three times with PBS and fixed with 4% paraformaldehyde in PBS for 30 minutes at room temperature. Cover slips were mounted on the slides with Prolong®Gold antifade reagent (Invitrogen, USA), and fluorescent intensity was detected using a TCS SP2 Confocal Laser Scanning Microscope (Leica Microsystems, Wetzlar, Germany).[24] Confocal images were obtained at 488 nm with an argon-ion laser with objective lens at 20× with electronic zoom settings. To quantify the cellular uptake of nanoparticle levels, flow cytometry was used.[25] HAs were treated with different concentrations of fluorescein isothiocyanate (FITC)-tagged nanoformulation (50, 100, and 200 µg/mL). The cells were then harvested at 24 hours after treatment and were counted; equal amounts of cells (1×10^6) were aliquoted in 12×75 mm polystyrene falcon tubes (catalog 352058; BD Biosciences, San Jose, CA, USA) and fixed with Cytofix solution (BD Bioscience). Cells were acquired on an Accuri C6 flow cytometer (BD Accuri, Ann Arbor, MI, USA) and analyzed with FlowJo software (Tree Star, Inc., Ashland, OR, USA). A total of 10,000 events were collected for each sample. Cells were gated on the basis of cells with and without nanoformulation controls. Cells positive for nanoformulation are shown in Figure 8 as colored histograms with shifted mean fluorescence intensity (MFI) compared with controls.

In vitro BBB preparation and transmigration assay

Primary human brain microvascular endothelial cells and HA cells were cultivated as per the provider's recommendations (ScienCell Research Laboratories, CA, USA). The BBB model was established as described by Persidsky et al.[26] In brief, the in vitro BBB model was developed in a bicompartmental transwell culture plate (product 3415; Corning Life Sciences, Mexico). The upper chamber of this plate is separated from the lower one by a 10 µm thick polycarbonate membrane possessing 3.0 µm pores. In a sterile 24-well cell culture plate with a pore density of 2×10^6 pores/cm^2 and a cell growth area of 0.33 cm^2, 2×10^5 human brain microvascular endothelial cells and HAs were grown to confluence on the upper chamber and underside of the lower chamber, respectively. To access the effect of MNP nanoformulation on the integrity of the in vitro BBB model, after transmigration assay, paracellular transport of FITC-dextran was measured.[15] Briefly, 100 mg/mL FITC-dextran (Sigma-Aldrich, St Louis, MO, USA) was added to the upper chamber of the inserts and further incubated for 6 hours. Samples were collected from the bottom chamber after 6 hours, and relative fluorescence was measured at excitation wavelength 485 nm and emission wavelength 520 nm, using a Synergy HT multimode microplate reader (BioTek Instruments, Inc., Winooski, VT, USA) multimode microplate reader instrument. FITC-dextran transport was expressed as percentage FITC-dextran transported across the BBB into the lower compartment compared with negative control. Intactness of in vitro BBB was determined by measuring the transendothelial electrical resistance (TEER), using Millicell ERS microelectrodes (Millipore). Transmigration study of drug-loaded MNP was conducted on the fifth or sixth day of the BBB culture, when ideal integrity of this membrane was achieved, as established by TEER measurement. MNP formulation was added to the apical chamber and incubated at 37°C in the presence or absence of a magnetic force of 0.08 T placed externally, below the transwell basolateral chamber. MNP nanoformulation was collected from lower chambers at 6 hours, and percentage transmigration was analyzed at different points, using an ammonium thiocyanate-based photometric assay.[18]

Cytotoxicity assay

Cytotoxicity was assessed by MTT cell viability assay, using a CellTiter 96® Aqueous one-solution cell proliferation assay kit (catalog G3580; Promega, USA).[19] HAs were seeded in 96-well tissue plates at a density of 5×10^3 cells per well. After 24 hours of incubation at 37°C, culture medium was replaced with 100 µL fresh media containing different concentrations of Fe_3O_4 (50–250 µg/mL). Twenty microliters MTT solution (5 mg/mL in PBS) were added into each well after 24 hours posttreatment and incubated at 37°C for 2 hours. Finally, 100 µL stop solution (20% sodium dodecyl sulfate in 50% dimethyl formamide) was added into each well, and absorbance was recorded at 550 nm by a microplate reader (Synergy HT; BioTek Instruments, Inc.).

Activation of latent HIV, using vorinostat and in vitro antiviral efficacy of the nanoformulation

To confirm the activation of latent cells and check the antiviral efficacy of the drug after the magnetic-triggered release process, we conducted a p24 antigen estimation. The cells were activated by treating them with polybrene (10 µg/mL) for 6 hours before the infection. HAs (10×10^6 cells) were infected with HIV-1Ba-L (catalog #510; National Institutes of Health AIDS Research and Reference Reagent Program) overnight, as described by Atluri et al,[24] washed with PBS and returned to culture with and without standard drug solution (tenofovir and vorinostat) or drug-loaded nanoformulation at equimolar concentrations. The culture supernatants were quantitated for p24 antigen, using an enzyme-linked immunosorbent assay kit (ZeptoMetrix, NY, USA) on the third, fifth, and seventh days postinfection, expressed as picograms per milliliter.

Statistical analysis

Experiments were performed at least three times in duplicate, unless otherwise indicated in the figure legends. The values obtained were averaged, and data are represented as the mean ± standard error. All the data were analyzed using GraphPad Prism software. Comparisons between groups were performed using one-way analysis of variance. Differences were considered significant at $P\leq0.05$.

Results

Formulation characterization and drug-release kinetics

Ultrasmall magnetite nanoparticles were prepared and characterized for size, shape, crystallinity, and drug loading. Transmission electron microscopy shows that nanoparticles were in the range of 10±3 nm, as shown in Figure 3A, with excellent dispersion properties (polydispersion index >0.81) in aqueous medium. In addition, the effect of drug loading and LbL deposition on MNP with respect to its hydrodynamic diameter also was determined (data shown in Figure S1). Magnetic hysteresis loops for MNP displayed strong magnetic behavior (exhibited by a superparamagnetic property with no coercivity and remanence), when measured between +1,200 and −1,200 Oersted at room temperature (as shown in Figure 3B). The crystal structure of synthesized magnetite particles was confirmed by X-ray diffraction spectroscopic measurement (Figure 3C). The X-ray spectrum consists of magnetite-specific peaks that correspond to 220, 311, 400, 511, and 440 planes. The encapsulation efficiency of tenofovir-loaded (35%±8%) and vorinostat-loaded (25%±8%) uncoated MNPs were calculated.

LbL assembly deposition was confirmed using zeta potential analysis; results show that the zeta-potential value for uncoated MNPs coated with tenofovir was +8.62±1 mV, which reversed on adsorption of drug DS coating to −29.3±3 mV and kept on reversing on subsequent layer deposition, as shown in Figure 3D, thus confirming that layer deposition is taking place, as desired and predicted. Results showed (Figure 3E) that application of 1 layer of DS leads to 1.9 times (32–62.5 µg/mg MNPs) higher drug encapsulation and, in the case of 2 bilayers (2BL), loading increases to 2.8 times (32–90.7 µg). The pharmacokinetic release studies show that uncoated MNPs release 100% drug in 4 and 7 hours, respectively, for tenofovir and vorinostat. The application of LbL assembly (1 layer and 2BL) increases the tenofovir release duration from 48 to 120 hours, as shown in Figure 4 (inset shows the initial 4 hour burst release data for all type nanoformulations). To confirm the structural and functional integrity of the drug after the release process, mass spectrometry analysis (details given in Figure S2) of the drug (tenofovir) was performed before (standard drug) and after the release (results shown in Figure S3).

In vitro BBB characterization and formulation transmigration assay

The BBB transmigrability of the plain MNPs and MNPs-2BL drug-loaded nanoformulation was evaluated using an in vitro human BBB model. The intactness of grown BBB was determined by TEER values. After the TEER determination, MNP nanocarriers were subjected to different wells, either in the presence or the absence of external magnetic force. As shown in Table 1, initial TEER values of all treatment groups were

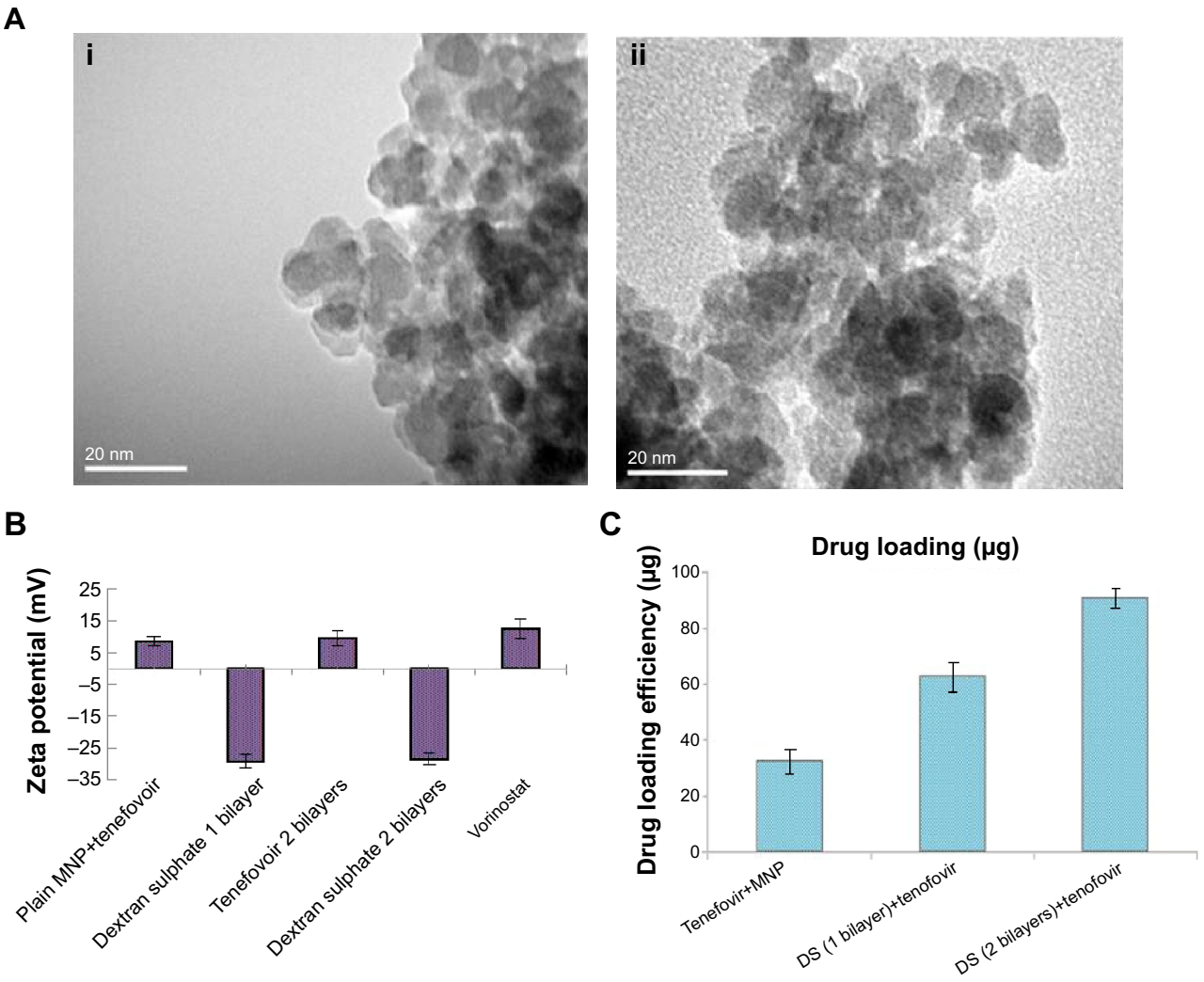

Figure 3 Characterizations of magnetic nanoparticle nanoformulation.
Notes: (**A**) Transmission electron microscopy of magnetic nanoparticles. (**i**) Uncoated magnetic nanoparticles. (**ii**) Two bilayer drug-loaded magnetic nanoparticles with ([magnetic nanoparticle+tenofovir]$_2$+vorinostat). (**B**) Zeta potential analysis for confirmation of drug-layer deposition. (**C**) Effect of dextran sulphate sodium layer coating with respect to the tenofovir loading profile.
Abbreviations: DS, dextran sulphate sodium; MNP, magnetic nanoparticles.

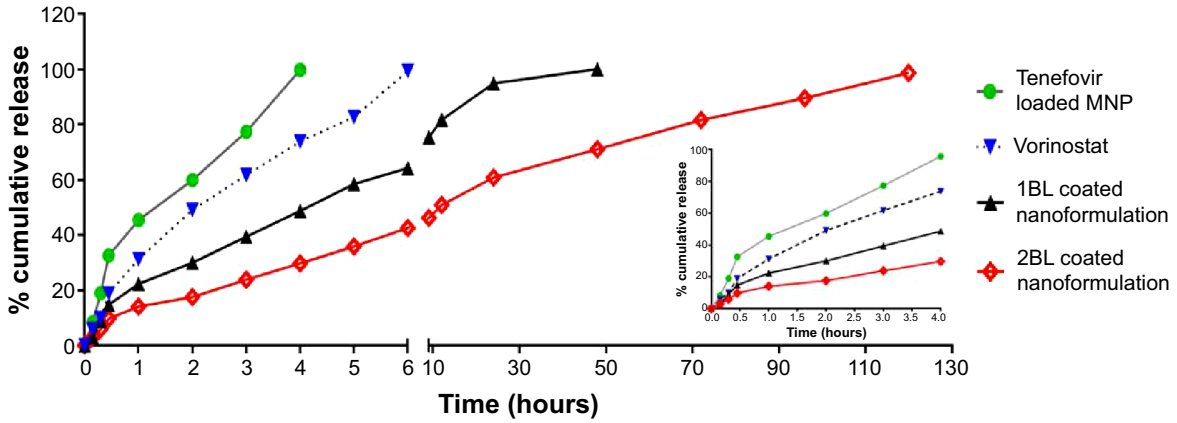

Figure 4 Pharmacokinetic release data.
Notes: Comparative cumulative release profile of uncoated tenofovir, uncoated vorinostat, and dextran-coated (1 layer [1BL] and two bilayers [2BL]) nanoformulation in phosphate-buffered saline (pH, 7.4) at 37°C. Inset shows the initial burst release profile at 4 hours for all the nanoformulations.
Abbreviation: MNP, magnetic nanoparticle.

Table 1 Transendothelial electrical resistance values of the in vitro blood–brain barrier model before and after treatment of nanocarriers (coated and uncoated) in the presence and absence of external magnetic force

Transendothelial electrical resistance values, ohms/cm^2	Untreated well (control)	Plain magnetic nanoparticles	Drug-loaded magnetic nanoparticles	Two bilayer coated magnetic nanoformulation
Before treatment	198.2±7.9	201.2±6.5	197.2±5.9	194.3±5.6
After magnetic treatment	192.6±5.8	198.4±7.5	190.2±6.2	196.2±4.3

similar to standard 200±5 ohms/cm^2. A schematic of proposed mechanisms of transmigration across BBB has been depicted in Figure 1. As expected, there was no difference found in the formulations value (results shown in Table 1) when compared with uncoated and unloaded MNP carriers.

Formulation ability with respect to BBB transmigration was verified by measuring the iron concentration after application of the external magnetic field. As evident from Figure 5A, 40%±3% of plain MNP versus 31.8%±3.5% of final nanoformulation ([MNP+tenofovir]$_2$+vorinostat) crosses the BBB in the presence of 0.8 T magnetic fields in 6 hours.

Without application of external magnetic force, only 2%±1.5% of the formulations were able to cross the BBB in 6 hours (result not shown). Furthermore, the integrity of BBB was evaluated using paracellular transport of FITC-dextran, as described earlier,[27] where the FITC molecule was used as a detection moiety to confirm the membrane intactness. Figure 5B shows that only 7–8%±2% of the FITC molecule was detected in the transmigration (apical to basolateral chamber) in the entire nanoformulation treatment sample compared with ~100% in the case of negative control (without any BBB cells), thus showing that transmigration of MNP nanoformulation under external magnetic field does not affect the BBB integrity

In vitro cytotoxicity and cellular uptake studies

To evaluate the cytotoxicity of nanoformulation, we performed the MTT cytotoxicity assay on HAs. Results show (Figure 6) that treatments with different concentrations (50–200 µg/mL) of nanoengineered MNP nanoformulation do not show any cytotoxicity, and the percentage of viable cells was similar to untreated control, suggesting that doses of nanoformulation are nontoxic and have no significant safety concerns. Experiments were also conducted in neuronal cells and peripheral cells, and there were no cytotoxic effects observed (data shown in Figure S4 for neuronal cells).

In addition, the qualitative and quantitative analysis of formulation, in terms of cellular uptake, was performed

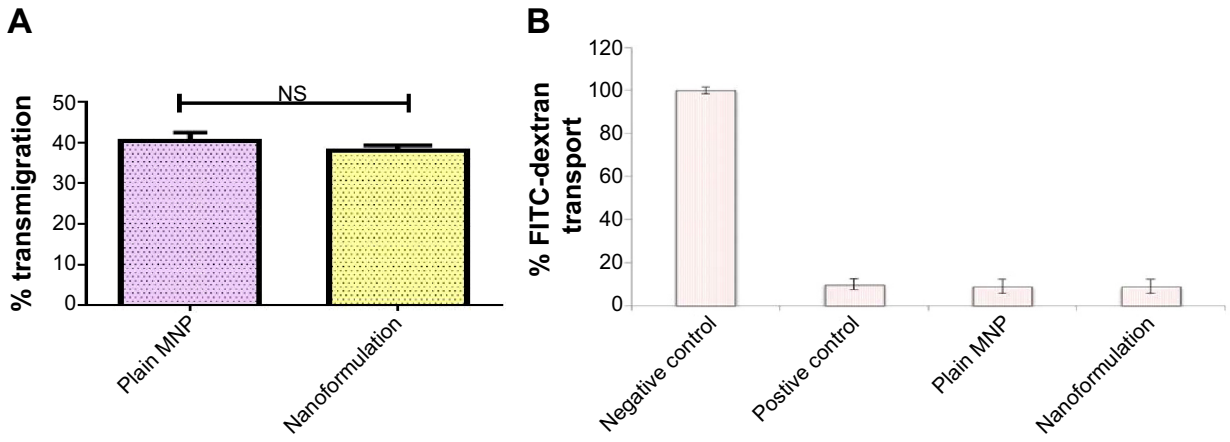

Figure 5 In vitro blood brain barrier model characterization.
Notes: (**A**) Magnetic nanoparticle (MNP) nanoformulation transmigration across an in vitro blood–brain barrier model. Magnetic nanoformulation was added in the upper chamber of the blood–brain barrier model with a magnet placed underneath for the duration of experiment. At 6 hours after plating, migrated plain MNPs and nanoformulations were calculated for iron content in the lower chamber. Results are expressed as mean ± standard error of three independent experiments. Statistical significance was determined using unpaired Student's *t*-test. (**B**) Effect of nanoformulation on fluorescein isothiocyanate-dextran transport in the blood–brain barrier model. Fluorescein isothiocyanate-dextran transport was measured in blood–brain barrier model after 6 hours of magnetic treatment. FITC-dextran was added on the upper chamber of the insert. After 6 hours of incubation, relative fluorescence units from the basal chambers of the inserts were measured. Results were expressed as percentage fluorescein isothiocyanate-dextran transport with respect to the untreated control cultures (negative control = no cell and positive control = with cells) and represented as mean ± standard error of independent experiments. NS indicates when *P*-value was found to be more than 0.05, then the result would be considered statistically not significant.
Abbreviation: FITC, fluorescein isothiocyanate.

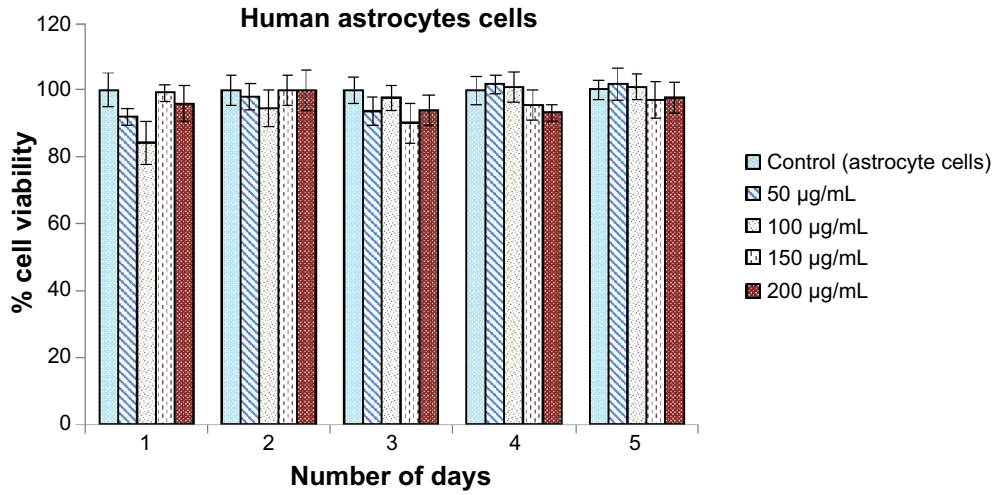

Figure 6 Cell viability of human astrocytes with magnetic nanoparticle nanoformulation.
Notes: Results show the percentage of cells viable after treatment with different concentrations of nanoformulation (50–200 µg/mL) for 24 hours.

using the same concentrations (50–200 µg/mL). Confocal microscopy was used to visualize the MNP nanoformulation particle uptake at different points (range, 6–24 hours). Figure 7 represents the cellular uptake of formulation in HAs after 6 hours of nanoformulation treatment at 100 µg/mL concentration.

For quantitative analysis, a flow cytometer was used. Our results show a concentration-dependent increase in the percentage of cells positive for FITC-tagged nanoformulation: As the concentration increased from 50 to 200 µg/mL, there was 1.25-fold (ie, 35.7% to 44%) increase in the percentage of cells positive for FITC-tagged nanoformulation, as shown in Figure 8 after 24 hours of treatment. Furthermore, when we analyzed the MFI, as shown in the legend, there was a significant concentration-dependent increase in MFI; for instance, a MFI of 59,395 was observed for 50 µg/mL

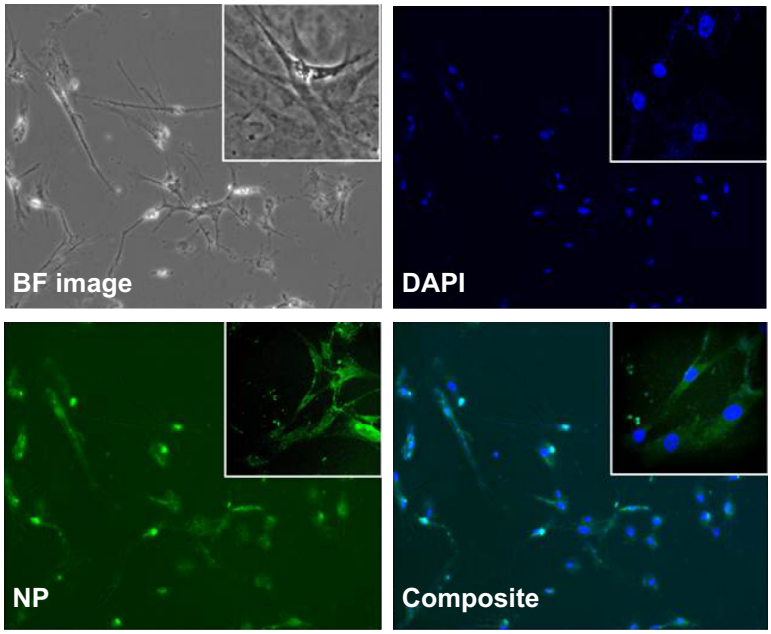

Figure 7 Cell uptake of fluorescein isothiocyanate-tagged magnetic nanoparticle nanoformulation (concentration, 100 µg/mL) in primary human astrocyte after 6 hours of treatment.
Notes: Composite image shows green (drug-loaded 2-layer formulation) and blue (cell nuclei) fluorescence inside the cells, and thus confirms the cellular uptake of the nanoformulation. Images were taken at 10× magnification (inset image magnifications, 20×), using fluorescence microscopy (Leica, Wetzlar, Germany).
Abbreviations: BF, bright field image; DAPI, 4′,6-diamidino-2-phenylindole, dihydrochloride; NP, nanoparticle.

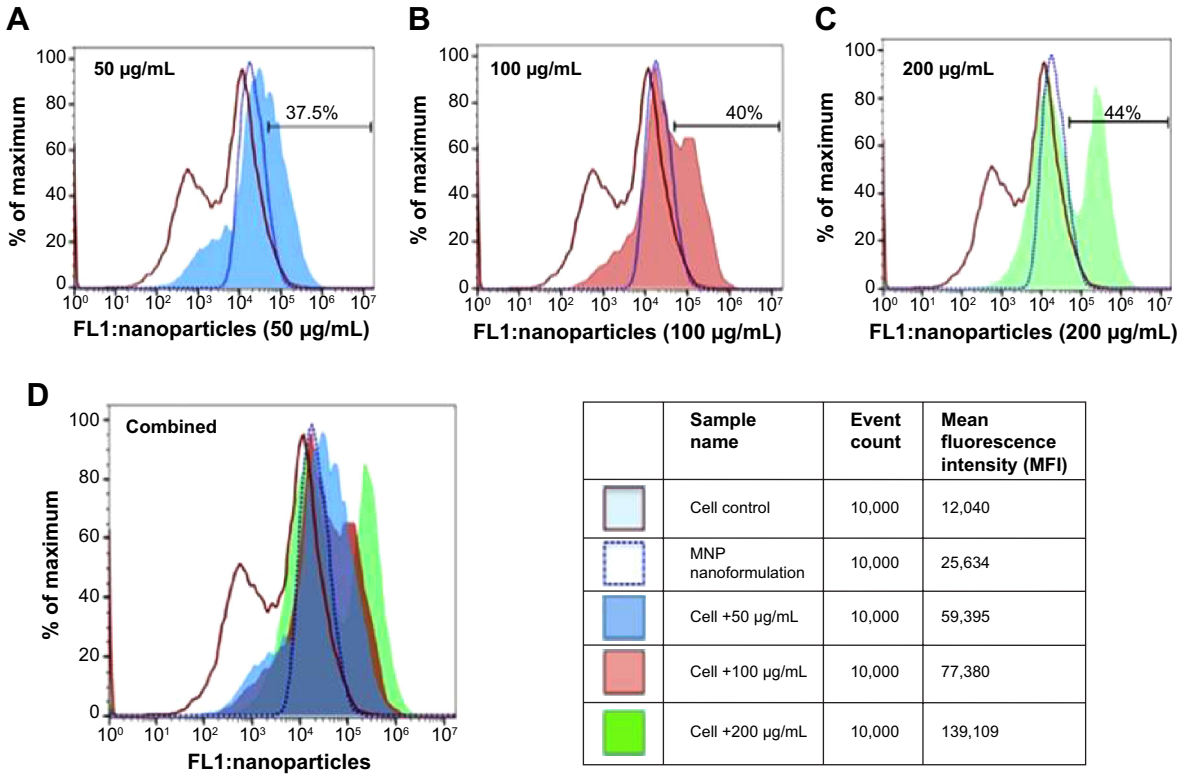

	Sample name	Event count	Mean fluorescence intensity (MFI)
	Cell control	10,000	12,040
	MNP nanoformulation	10,000	25,634
	Cell +50 µg/mL	10,000	59,395
	Cell +100 µg/mL	10,000	77,380
	Cell +200 µg/mL	10,000	139,109

Figure 8 Quantitative analysis of fluorescein isothiocyanate-tagged magnetic nanoparticle nanoformulation after 24 hours of treatment in primary human astrocytes by flow cytometry.

Notes: Data suggest that an increase in concentration from 50 to 200 µg/mL leads to an increase in the percentage of cells positive for fluorescein isothiocyanate-tagged nanoformulation, as well as an increase in mean fluorescence intensity. Ten thousand events were collected for each sample. Cells were gated on the basis of cells without nanoformulation (brown line histogram) and nanoformulation alone (blue dotted-line histogram) controls. Cells positive for nanoformulation are shown as colored histograms with shifted mean fluorescence intensity compared with controls. Colored histograms on (**A**–**C**) represent cells treated with 50 (blue), 100 (red), and 200 (green) µg/mL fluorescein isothiocyanate-tagged nanoformulation, which shows a 35.7%, 40%, and 44% increase in cells positive for nanoformulation and 59,395, 77,380, and 139,109 mean fluorescence intensity, respectively. Histograms on (**D**) show an overlay of all three concentrations (50, 100, 200 µg/mL).

Abbreviations: FL, fluorescence; MNP, magnetic nanoparticle.

concentration, which increased to 139,109 (ie, 2.3-fold) when concentration was increased to 200 µg/mL. Overall, it is relevant to point out that the increase in MFI correlated with an increase in the percentage of cells positive for FITC-tagged nanoformulation, and that both increases were concentration-dependent.

Latency-breaking and in vitro antiviral efficacy of the nanoformulation

Latency-breaking and antiviral efficacy of the nanoformulation was determined via quantification of p24 antigen in the HA infection model.[19] Our group reports for the first time that vorinostat significantly activates latent HIV infection in the neuronal cells.[28] Different concentrations (0.5–5 µM) of vorinostat (solution phase) were tested for the latency-breaking ability; the results showed that a 1 µM concentration yields a significant difference in p24 value (data shown in Figure S5) and was used for the final formulation development. To confirm the efficacy of the nanoformulation after the magnetic-triggered release process after 24 hours, we conducted a p24 viral replication assay, the results of which showed (Figure 9) that standard tenofovir (1 mg/mL solution), and MNPs-2BL nanoformulation showed equal p24 inhibition efficacy after the third day postinfection, thus suggesting that the integrity and efficacy of the drug are not lost after external magnetic application.

The results show a good latency-breaking ability for vorinostat-loaded MNPs (20.5% increase) when compared for p24 levels, with respect to positive control (HIV-infected HA cells), as shown in Figure 10 on day 1 of nanoformulation treatment. The sustained-release ability of the finally assembled nanoformulation ($[MNP+tenofovir]_2$+vorinostat) was also evaluated over a treatment period of 5 days in the HA model.

Our results showed that there was a significant suppression of viral load (~33%; 390–260 pg/mL) reduction of p24 level found after 7 days of HIV infection with 5 days of nanoformulation treatment, which clearly shows that drug

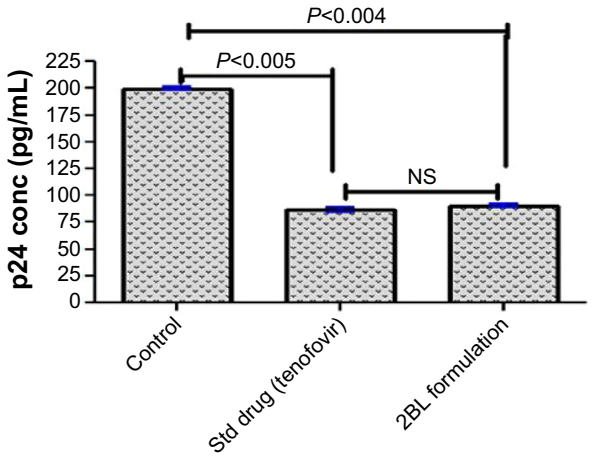

Figure 9 p24 study to prove that the magnetically triggered release does not affect the inhibition efficacy of the drug (tenofovir) in HIV replication.
Notes: Release drug and standard drug (1 mg/mL) used for efficacy assay in human astrocytes. Treatment was done for 24 hours, and results were analyzed via p24 antigen estimation, using enzyme-linked immunosorbent assay on the fifth day of infection and expressed as picograms per milliliter.
Abbreviations: 2BL, 2 bilayers; Std, standard; NS, not significant.

is getting released in sustained manner over a period of 5 days and is able to activate latent cells and suppress the viral replication.

Discussion

Adherence to dosing regimens is a critical issue for HIV treatment and its prevention. It has been hypothesized that the development of approaches eliminating or reducing the effect of individual adherence could increase the efficacy of treatment strategies and provide for the prevention of HIV transmission. Considering this scenario, there is a need to develop new and innovative sustained-release antiviral formulations for better treatment of HIV (peripheral or central nervous system) disease and the prevention of HIV transmission and acquisition. Magnetite (Fe_3O_4) is the most commonly used MNP in the field of biomedicine, mainly because of its biocompatibility. In this study, ultrasmall MNPs were developed by the coprecipitation method (the main advantage of this method is its circumstance-friendly and cost-effective method of preparation on the nanoscale) and tested for their drug-loading, in vitro release pharmacokinetics, cytotoxicity, and in vitro antiviral replication efficacy in central nervous system cells. The most important parameters affecting release behavior were identified and optimized. The superparamagnetism can be used for simultaneous monitoring and quantitation of MNP (specific or nonspecific) distribution to various tissues.

Distribution of charge on the surface of synthesized MNPs was determined by measuring the zeta potential. The zeta-potential values clearly demonstrated that the surface charge of the MNPs reverses on coating of alternately charged moieties (tenofovir/DS coating), proving that multilayer build-up is taking place. The desired system is expected to achieve complete release of the drug in 5–7 days to overcome the problem of frequent dosing and better patient adherence. To achieve 100% drug release over a period of 1 week with zero-order release kinetics, different amounts of tenofovir were used for loading. It was observed that drug loading of MNPs does not increase with increasing the drug amount to the nanoparticles. In most cases, drugs are either directly immobilized or loaded on the nanocarrier surface

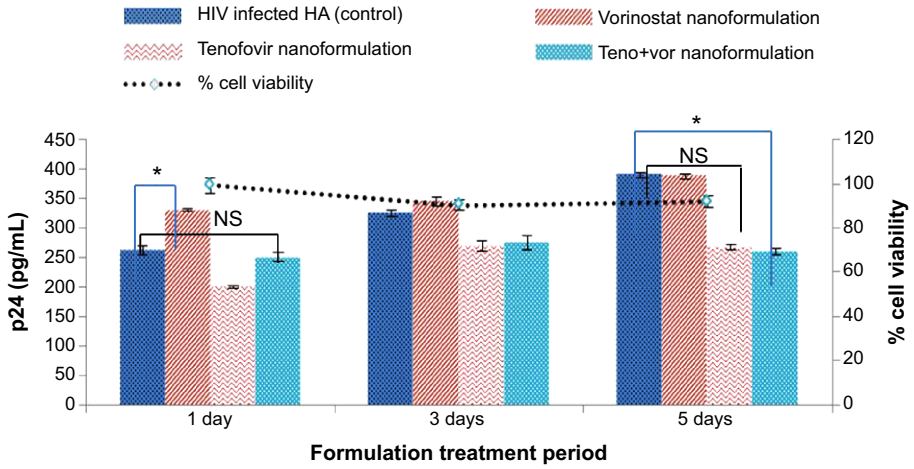

Figure 10 Evaluation of antiviral efficacy of nanoformulation in suppressing p24 antigen levels in HIV-infected human astrocytes.
Notes: Nanoformulations were added on the second day after HIV infection (HIV-1BaL) in equimolar concentration. Supernatants were evaluated on third, fifth, and seventh day postinfection for p24 levels and were checked for its efficacy, along with its percentage cell viability, using MTT assay. Simultaneous incorporation of tenofovir and vorinostat into the magnetic nanoparticles' nanoformulation leads to latent virus activation and inhibits viral spread almost comparable to tenofovir nanoformulation. Viral p24 protein in the culture supernatant was measured by enzyme-linked immunosorbent assay. Error bars indicate the standard deviation of triplicate data points and are representative of at least three experiments. Dotted lines represent the percentage cell viability; each point represents treatment period. *If mean *P*-value was found to be less than 0.05, then the result would be considered statistically significant.
Abbreviations: HA, human astrocytes; Teno, tenofovir; Vor, vorinostat; NS, nonsignificant.

or tethered via adsorption or immobilization (coating) of organic/inorganic surfactants (eg, polyethylene glycol).[29,30] In either case, attached drugs are exposed to the external environment and possess the threat of rapid decomposition because of metabolic (enzymatic mainly) activity of the peripheral circulation (blood) before it could reach the target.[14,18] Even though the nanoparticles have a high surface area, one of the major limitations in drug delivery is their low drug-loading capacity, which could be a problem in the development of long-term or sustained-release formulations.

To avoid the abovementioned problems, scientists have used a hybridization strategy in which nanoparticle formulation is encapsulated in liposomes,[18,31] and this nanoformulation has developed as a possible solution, but the limitation with this technique is that it increases the size of nanoformulation up to +100 nm, which makes the formulation less able to cross the BBB.[32–34] Considering these limitations, we have proposed, for the first time, the use of LbL methodology[23,35] (spontaneous adsorption of alternating layers of positively and negatively charged species). This technique is simple, fast, and versatile and helps in loading more drugs as a result of the electrostatic interaction between oppositely charged layers. The rate of release can also be adjusted through shell thickness, which can be controlled according to layer numbers. Another advantage of this thin film nanoengineered architecture deposition is the precision of layer thickness control that is within the range of 3–5 nm (each layer), which helps in maintaining the size of nanoparticles within the desirable range.

Therefore, to achieve sustained drug release, a LbL self-assembly technique was applied to the MNPs, helping to reduce the initial burst and prolonging the period of release in the induction phase without significantly affecting the release rate. Our results demonstrate that the zeta potential of nanoparticle formulation reversed on the addition of oppositely charged polyelectrolyte and drug $(DS/tenofovir)_2$ coatings, causing greater stability of nanoparticles, as indicated by the greater negative and positive charges. Electrostatic interactions between the nanoparticles and the polyelectrolytes are the main driving force for multilayer build-up. These interactions seem to be strong enough; otherwise, the adsorbed layers would be removed on the adsorption process of the next polyelectrolyte layer, as evident by zeta-potential analysis. Results showed that LbL significantly reduced the tenofovir initial burst threefold and increased the duration of drug release (30 times) in the induction phase (4 versus 120 hours). In the case of vorinostat-uncoated MNP release, there was a slow release of vorinostat because of its low water solubility (7 hours) compared with that of uncoated MNPs loaded with tenofovir (4 hours).

Cytotoxicity testing of the nanoformulation is highly recommended and is considered one of the most fundamental tests for biocompatibility. The aim of cytotoxicity studies is to evaluate the in vitro biocompatibility of a drug-loaded polyelectrolyte-coated nanoformulation in different brain cells. Different cellular aspects were analyzed to determine the cell viability in HAs, such as cell uptake, adhesion, proliferation, and morphology. The results provided good evidence of adhesion, growth, and morphology, with more than 95% of cell viability in cases of all different concentrations of nanoformulation. Flow cytometer analysis of cellular uptake shows a concentration-dependent increase in cell uptake, which is evident from the increase in mean fluorescence intensity and increased percentage of cells positive for FITC-tagged nanoformulation. Furthermore, the effect of the magnetic field on the transmigration ability and BBB integrity of the formulation was evaluated, and results show there was no damage to the BBB and that more than 40% of the nanoformulation crosses the BBB only after the application of 6 hour magnetic field. To achieve higher transmigration of the formulation, we have optimized the important parameters of magnetic field and time of application. The results demonstrate the ability of our nanoformulation system to be efficiently taken up into the cells and provide a platform with which we can effectively deliver our cargo of interest (ie, an HIV-latency activator [vorinostat] and nucleotide reverse transcriptase inhibitor [tenofovir]). The integrity of the release drug after the magnetic field was evaluated using mass spectroscopy and checked for its antiviral replication efficacy. Our results demonstrate that free standard drug displays inhibition equal to that of the released nanoformulation. To test the ability of nanoformulation ($[MNP+tenofovir]_2$+vorinostat) to activate latent virus, we used the HA cell culture system. In addition, the long-term sustained-release behavior was studied directly in the HIV-infected HA cell culture system. Results were very positive; nanoformulation can effectively control virus spread up to 5 days in a continuous manner, while at the same time being able to stimulate latent HIV expression in HA cells, as evident in the results.

Conclusion

In conclusion, the current work is an in vitro proof of study demonstrating that latency-breaking agents can be packaged into nanoparticles in conjunction with an antiretroviral drug. We successfully established the application of the LbL assembly technique by achieving long-term release (5 days) across the BBB in a sustained manner. Further, we combined the synergistic effect of vorinostat and tenofovir

in a single nanoformulation and demonstrated the ability of nanotechnological approaches to provide improved methods for activating latent viruses and killing them simultaneously. Novel drug delivery systems such as the one described here may enhance the future of HIV therapy by using combination therapy of ARV drugs (ie, [nucleotide reverse transcriptase inhibitor+nucleotide reverse transcriptase inhibitor+protease inhibitor] or [nucleotide reverse transcriptase inhibitor+protease inhibitor+integrase inhibitor]) to achieve better efficacy and complete the eradication of the virus from the central nervous system. In the future, in vivo studies will be performed using the HIV-infected severe combined immunodeficiency mouse model to assess the free drug amount (microdialysis) present in the brain parenchyma to evaluate the therapeutic efficacy of the nanoformulation.

Acknowledgments

We acknowledge receiving financial support from National Institutes of Health (grants 1R01MH085259 and R01DA034547-01) and the NIH-AIDS Research Program for the antiretroviral drug.

Disclosure

The authors report no conflicts of interest in this work.

References

1. Williams I, Churchill D, Anderson J, et al. British HIV Association guidelines for the treatment of HIV-1-positive adults with antiretroviral therapy 2012. *HIV Med*. 2012;13(suppl 2):1–85.
2. García de Olalla P, Knobel H, Carmona A, Guelar A, López-Colomés JL, Caylà JA. Impact of adherence and highly active antiretroviral therapy on survival in HIV-infected patients. *J Acquir Immune Defic Syndr*. 2002;30(1):105–110.
3. Nowacek A, Gendelman HE. NanoART, neuroAIDS and CNS drug delivery. *Nanomedicine (Lond)*. 2009;4(5):557–574.
4. Bangsberg DR, Perry S, Charlebois ED, et al. Non-adherence to highly active antiretroviral therapy predicts progression to AIDS. *AIDS*. 2001;15(9):1181–1183.
5. Adherence to HIV Antiretroviral Therapy. HIV InSite Knowledge Base Chapter; 2005 [reviewed January 2006]. Available from: http://hivinsite.ucsf.edu/insite?page=kb-03-02-09. Accessed December 20, 2014.
6. Kelly JA, Kalichman SC. Behavioral research in HIV/AIDS primary and secondary prevention: recent advances and future directions. *J Consult Clin Psychol*. 2002;70(3):626–639.
7. Martin LR, Williams SL, Haskard KB, Dimatteo MR. The challenge of patient adherence. *Ther Clin Risk Manag*. 2005;1(3):189–199.
8. Kovochich M, Marsden MD, Zack JA. Activation of latent HIV using drug-loaded nanoparticles. *PLoS ONE*. 2011;6(4):e18270.
9. Archin NM, Espeseth A, Parker D, Cheema M, Hazuda D, Margolis DM. Expression of latent HIV induced by the potent HDAC inhibitor suberoylanilide hydroxamic acid. *AIDS Res Hum Retroviruses*. 2009;25(2):207–212.
10. Thomas SA. Anti-HIV drug distribution to the central nervous system. *Curr Pharm Des*. 2004;10(12):1313–1324.
11. Ayre SG. New approaches to the delivery of drugs to the brain. *Med Hypotheses*. 1989;29(4):283–291.
12. Bhaskar S, Tian F, Stoeger T, et al. Multifunctional Nanocarriers for diagnostics, drug delivery and targeted treatment across blood–brain barrier: perspectives on tracking and neuroimaging. *Part Fibre Toxicol*. 2010;7(1):3.
13. Pardridge WM. Blood–brain barrier delivery. *Drug Discov Today*. 2007;12(1–2):54–61.
14. Sagar V, Pilakka-Kanthikeel S, Pottathil R, Saxena SK, Nair M. Towards nanomedicines for neuroAIDS. *Rev Med Virol*. 2014;24(2):103–124.
15. Saiyed ZM, Gandhi NH, Nair MP. Magnetic nanoformulation of azidothymidine 5′-triphosphate for targeted delivery across the blood–brain barrier. *Int J Nanomedicine*. 2010;5:157–166.
16. Varatharajan L, Thomas SA. The transport of anti-HIV drugs across blood-CNS interfaces: summary of current knowledge and recommendations for further research. *Antiviral Res*. 2009;82(2):A99–A109.
17. Boffito M, Jackson A, Owen A, Becker S. New approaches to antiretroviral drug delivery: challenges and opportunities associated with the use of long-acting injectable agents. *Drugs*. 2014;74(1):7–13.
18. Ding H, Sagar V, Agudelo M, et al. Enhanced blood–brain barrier transmigration using a novel transferrin embedded fluorescent magneto-liposome nanoformulation. *Nanotechnology*. 2014;25(5):055101.
19. Nair M, Guduru R, Liang P, Hong J, Sagar V, Khizroev S. Externally controlled on-demand release of anti-HIV drug using magneto-electric nanoparticles as carriers. *Nat Commun*. 2013;4:1707.
20. Pilakka-Kanthikeel S, Atluri VSR, Sagar V, Saxena SK, Nair M. Targeted brain derived neurotropic factors (BDNF) delivery across the blood–brain barrier for neuro-protection using magnetic nano carriers: an in vitro study. *PLoS ONE*. 2013;8(4):e62241.
21. Wohlfart S, Gelperina S, Kreuter J. Transport of drugs across the blood–brain barrier by nanoparticles. *J Control Release*. 2012;161(2):264–273.
22. Sun Y, Ma M, Zhang Y, Gu N. Synthesis of nanometer-size maghemite particles from magnetite. *Colloids Surf A Physicochem Eng Asp*. 2004;245(1–3):15–19.
23. Decher G. Fuzzy nanoassemblies: Toward layered polymeric multicomposites. *Science*. 1997;277(5330):1232–1237.
24. Atluri VSR, Kanthikeel SP, Reddy PV, Yndart A, Nair MP. Human synaptic plasticity gene expression profile and dendritic spine density changes in HIV-infected human CNS cells: role in HIV-associated neurocognitive disorders (HAND). *PLoS ONE*. 2013;8(4):e61399.
25. Toduka Y, Toyooka T, Ibuki Y. Flow cytometric evaluation of nanoparticles using side-scattered light and reactive oxygen species-mediated fluorescence-correlation with genotoxicity. *Environ Sci Technol*. 2012;46(14):7629–7636.
26. Persidsky Y, Stins M, Way D, et al. A model for monocyte migration through the blood–brain barrier during HIV-1 encephalitis. *J Immunol*. 1997;158(7):3499–3510.
27. Gandhi N, Saiyed ZM, Napuri J, et al. Interactive role of human immunodeficiency virus type 1 (HIV-1) clade-specific Tat protein and cocaine in blood–brain barrier dysfunction: implications for HIV-1-associated neurocognitive disorder. *J Neurovirol*. 2010;16(4):294–305.
28. Atluri VS, Pilakka-Kanthikeel S, Samikkannu T, et al. Vorinostat positively regulates synaptic plasticity genes expression and spine density in HIV infected neurons: role of nicotine in progression of HIV-associated neurocognitive disorder. *Mol Brain*. 2014;7(1):37.
29. Jayant R. Layer-by-Layer (LbL) assembly of anti HIV drug for sustained release to brain using magnetic nanoparticles. *J Neuroimmune Pharmacol*. 2014;9(1):25.
30. Jayant RD, McShane MJ, Srivastava R. Polyelectrolyte-coated alginate microspheres as drug delivery carriers for dexamethasone release. *Drug Deliv*. 2009;16(6):331–340.
31. Kargol A, Malkinski L, Caruntu G. Biomedical applications of multiferroic nanoparticles. In: Malkinski L, editor. *Advanced Magnetic Materials*. Rijeka, Croatia: Intech; 2006:89–118.

32. Caraglia M, De Rosa G, Salzano G, et al. Nanotech revolution for the anti-cancer drug delivery through blood–brain barrier. *Curr Cancer Drug Targets*. 2012;12(3):186–196.
33. De Rosa G, Salzano G, Caraglia M, Abbruzzese A. Nanotechnologies: a strategy to overcome blood–brain barrier. *Curr Drug Metab*. 2012; 13(1):61–69.
34. Kaushik A, Jayant RD, Sagar V, Nair M. The potential of magneto-electric nanocarriers for drug delivery. *Expert Opin Drug Deliv*. 2014; 11(10):1635–1646.
35. Jayant RD, Srivastava R. Dexamethasone release from uniform sized nanoengineered alginate microspheres. *J Biomed Nanotechnol*. 2007; 3(3):245–253.

Supplementary materials

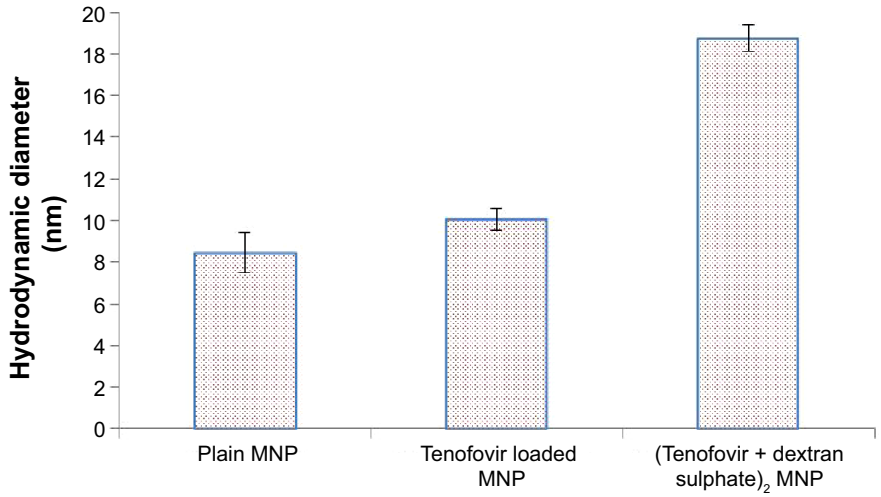

Figure S1 DLS measurement of hydrodynamic diameter with respect to drug loading and layer-by-layer assembly deposition.
Abbreviations: DLS, dynamic light scattering; MNP, magnetic nanoparticle.

Source parameter	Value
Drying gas temp	325°C
Gas flow	10 psi
Nebulizer	30 psi
Sheath gas heater	375°C
Sheath gas flow (l/min)	11
Nozzle voltage	0 V
Capillary voltage (Vcap)	3,500 V
Scan parameters	
Mass range	50–1,000
Scan time	350 ms
Fragmentor voltage	135 V
Cell acelerator voltage	4 V
Polarity	Negative

Figure S2 Mass spectrometry analysis.
Note: Mass spectrometry instrumental parameters used for the LC/MSD analyses (General Screening Method).
Abbreviations: LC/MSD, liquid chromatography–mass spectrometry data; temp, temperature; Vcap, capillary voltage; min, minute.

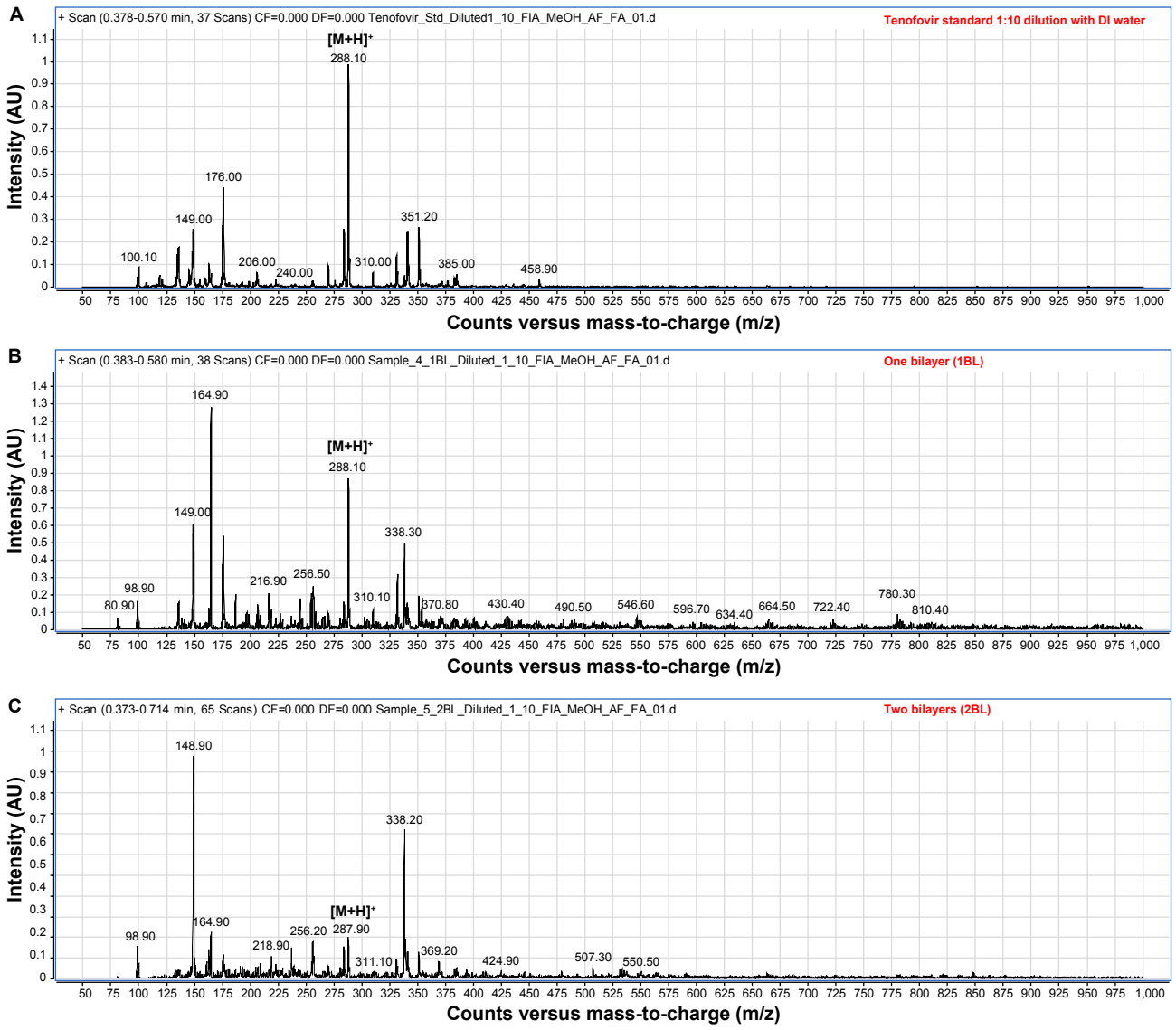

Figure S3 Mass spectroscopy analysis.

Notes: The number of counts versus the mass-to-charge ratio (standard peak of 288) for (**A**) the standard free tenofovir (1:10 water dilution); (**B**) released tenofovir from 1 bilayer formulation (MNP+tenefovir+dextran sulphate); and (**C**) released tenofovir from 2 bilayers formulation ([tenofovir+dextran sulphate]$_2$+vorinostat). $[M+H]^+$ indicates protonated molecular ions of the formula in positive ionisation mode.

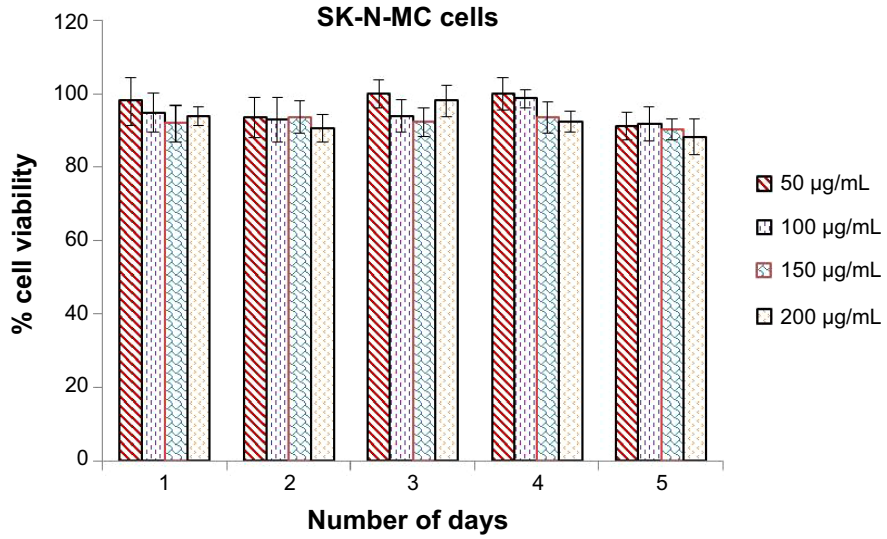

Figure S4 Cell viability of neuronal cells (SK-N-MC cells) with MNP nanoformulation.
Note: Results show the percentage of cells viable after treatment with different concentrations of (50–200 µg/mL) for 24 hours.
Abbreviation: MNP, magnetic nanoparticles.

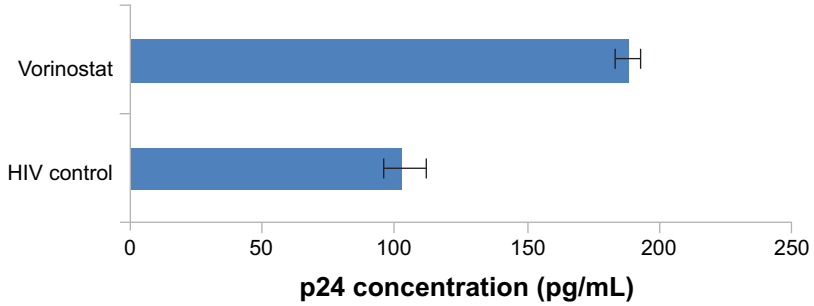

Figure S5 p24 study to show effect of standard (free drug) vorinostat on HIV replication in human astrocytes.
Note: Different ranges of vorinostat (0.5–5 µm) were used; results show maximum p24 value at 1µM concentration, which is used for the nanoformulation development.